Electronic Supplementary Information

Stretchable Crumpled Graphene Photodetector with Plasmonically-enhanced Photoresponsivity

Minsu Kim[a‡], Pilgyu Kang[b‡], Juyoung Leem[b‡], and SungWoo Nam*[a,b]

[1]Department of Materials Science and Engineering,
University of Illinois at Urbana-Champaign, Urbana, Illinois 61801, United States
[2]Department of Mechanical Science and Engineering,
University of Illinois at Urbana-Champaign, Urbana, Illinois 61801, United States

*Corresponding Author: swnam@illinois.edu

Fabrication of crumpled graphene-AuNPs hybrid structures

Graphene was synthesized on a 25 µm thick copper (Cu) foil (Alfa Aesar, MA) by a low-pressure chemical vapour deposition (LPCVD) system (Rocky Mountain Vacuum Tech Inc., CO). Before the synthesis, the copper foil was immersed in hydrochloric acid for 10 minutes to remove a native copper oxide layer and impurities on the surface. Then, the foil was cleaned with deionized (DI) water and isopropyl alcohol (IPA), and placed into the CVD chamber. The CVD chamber was vacuumed below 1 mTorr, and temperature was raised up to 1050°C under hydrogen (H_2) gas atmosphere at 150 mTorr. The foil was annealed at 1050°C for 35 minutes to refine the surface and grow the grain size of Cu. Then, the pressure was increased to 520 mTorr with an inflow of methane (CH_4) gas for 2 minutes to synthesize graphene. Then, the chamber was cooled under an inflow of Argon (Ar) gas at 330 mTorr. After the synthesis, graphene formed at the back side of the Cu foil was removed by oxygen plasma etching (Diener GmbH, Germany). The quality of graphene was examined by Raman spectroscopy (Renishaw, UK).

A 3 nm-thick gold (Au) thin film was deposited on the graphene on a Cu foil by a thermal evaporator (Nano 36, Kurt J. Lesker, PA) at a deposition rate of 0.1 Å/s. The Au film on a graphene/Cu foil substrate was annealed at 200°C to create Au nanoparticles (AuNPs) on the graphene surface. The graphene-AuNPs hybrid structure on a Cu foil was transferred onto a polydimethylsiloxane (PDMS) substrate to remove the Cu substrate. AuNPs on the graphene and the PDMS substrate were in contact. The Cu substrate was removed by ferric chloride ($FeCl_3$) aqueous solution. After Cu was completely etched, the hybrid film on the PDMS substrate was transferred by placing the hybrid film on the PDMS substrate onto a biaxially prestrained very high bond (VHB) film (3M™ VHB™ 4910, 3M, MN) and detaching the PDMS substrate. The

VHB film was biaxially pre-stretched by 350% in x-direction and 250% in y-direction. Finally, the pre-strained VHB film was released to obtain crumpled graphene-AuNPs hybrid structures.

Fabrication of a photodetector based on crumpled hybrid structures

To fabricate a photodetector consisting of a photoconductive channel and electrodes, the VHB film with the crumpled graphene-AuNPs hybrid structure was re-stretched 300% in the x-direction and 200% in the y-direction. Then, a 40 nm-thick Au film was thermally deposited with a shadow mask. By releasing the biaxial strains, the photodetector was obtained. Dimensions of channel length (L) and width (W) were ≈ 350 μm and ≈ 500-700 μm respectively. The dimensions were determined to be $L_{channel}>L_{beam}/2$ and $W_{channel} \approx W_{beam}$, so that the maximum possible photocurrent was measured. The beam size of an elliptical laser beam (λ_{light} = 532 nm, Thorlabs CPS532, NJ) was measured to be L_{beam} ~ 760 μm and W_{beam} ~1080 μm (Power ~3 mW through a 5X objective lens).

To fabricate a crumpled graphene photodetector, graphene synthesized on a Cu foil was transferred onto a PDMS film, and the Cu foil was etched away. The remaining fabrication processes were the same as the fabrication processes of the photodetector based on the crumpled hybrid structure. Dimensions of crumpled graphene channel length (L) and width (W) were ≈ 350 μm and ≈ 500-700 μm respectively, which were the same as channel dimensions of the crumpled hybrid structure.

To fabricate a flat graphene photodetector, the graphene on the PDMS substrate was transferred to an equi-biaxially pre-stretched (100%) VHB film. The pre-stretched VHB was permanently attached on a microscope glass slide so that the graphene was not crumpled. Next, a

40 nm-thick Au film was thermally deposited with a shadow mask to make source and drain contacts. Dimensions of flat graphene channel length (L) and width (W) were ≈ 350 μm and ≈ 500-700 μm respectively.

Analysis of crumple structure dimensions

Crumple wavelengths in the x-direction ($\lambda_{c,x}$) and the y-direction ($\lambda_{c,y}$) were determined by the analytical formula assuming biaxially crumpled structures[1]. A biaxially crumpled structure is mathematically expressed as $z = A \cdot \cos(2\pi x/\lambda_{c,x}) \cdot \cos(2\pi y/\lambda_{c,y})$, where A (= $h_c/2$, where h_c is crumple height) is crumple amplitude, and $\lambda_{c,x}$ and $\lambda_{c,y}$ are crumple wavelengths in x and y directions respectively.

$$\lambda_{c,x}{}^{-2} + \lambda_{c,y}{}^{-2} = \frac{1}{(2\pi \cdot h_f)^2}\left(\frac{3\bar{E}_s}{\bar{E}_f}\right)^{\frac{2}{3}} \tag{1}$$

$$\lambda_{c,x}{}^{-2} - \lambda_{c,y}{}^{-2} = \frac{1}{\left(2\pi \cdot h_f\right)^2}\left(\frac{3\bar{E}_s}{\bar{E}_f}\right)^{\frac{2}{3}}\left(\frac{3-\nu_f}{3+\nu_f}\right)\frac{\varepsilon_{pre,x}-\varepsilon_{pre,y}}{\varepsilon_{pre,x}+\varepsilon_{pre,y}-\left[\left(\frac{3\bar{E}_s}{\bar{E}_f}\right)^{\frac{2}{3}}\Big/2\left(1+\nu_f\right)\right]} \tag{2}$$

where h_f is film thickness, $\bar{E}_f$ $(= E_f/(1-\nu_f^2))$ and $\bar{E}_s$ $(= E_s/(1-\nu_s^2))$ are respective plane strain moduli of a film and a substrate, ν_f and ν_s are respective Poisson's ratios of a film and a substrate, and $\varepsilon_{pre,x}$ and $\varepsilon_{pre,y}$ are respective pre-strains in x and y directions.

The equations are simplified to calculate $\lambda_{c,x}{}^{-2}$ and $\lambda_{c,y}{}^{-2}$:

$$\lambda_{c,x}{}^{-2} = \frac{1}{2(2\pi\cdot h_f)^2}\left(\frac{3\bar{E}_s}{\bar{E}_f}\right)^{\frac{2}{3}}\left(1 + \left(\frac{3-\nu_f}{3+\nu_f}\right)\left(\frac{\varepsilon_{pre,x}-\varepsilon_{pre,y}}{\varepsilon_{pre,x}+\varepsilon_{pre,y}-\left[\left(\frac{3\bar{E}_s}{\bar{E}_f}\right)^{\frac{2}{3}}/2(1+\nu_f)\right]}\right)\right) \quad (3)$$

$$\lambda_{c,y}{}^{-2} = \frac{1}{2(2\pi\cdot h_f)^2}\left(\frac{3\bar{E}_s}{\bar{E}_f}\right)^{\frac{2}{3}}\left(1 - \left(\frac{3-\nu_f}{3+\nu_f}\right)\left(\frac{\varepsilon_{pre,x}-\varepsilon_{pre,y}}{\varepsilon_{pre,x}+\varepsilon_{pre,y}-\left[\left(\frac{3\bar{E}_s}{\bar{E}_f}\right)^{\frac{2}{3}}/2(1+\nu_f)\right]}\right)\right) \quad (4)$$

The thickness of a film, h_f, was assumed to be graphene thickness (0.34 nm). We assumed that AuNPs were not a composite layer on graphene because they were not a continuous layer and randomly distributed on graphene. Thus, only graphene was considered as a crumpled layer in our calculation. Poisson's ratios of graphene and VHB are 0.165[2-3] and 0.49 (manufacture's information of 3M™ VHB™ tape) respectively. The prestrains in the x-direction ($\varepsilon_{pre,x}$) and the y-direction ($\varepsilon_{pre,y}$) were 3.5 and 2.5 respectively. E_f is 1 TPa[3] and E_s is 2.2x10^2 kPa[4]. By inserting the above values into Eq. 3 and Eq. 4, $\lambda_{c,x}$ and $\lambda_{c,y}$ were calculated to be 298 nm and 346 nm respectively.

The amplitude of the structure (*A*) was calculated to be 209 nm by Eq. 5.

$$A = 4h_f\left(\frac{\bar{E}_f}{3\bar{E}_s}\right)^{\frac{1}{3}}\sqrt{\frac{1}{3-\nu_f}\left[\varepsilon_{pre,x}+\varepsilon_{pre,y}-\left[\left(\frac{3\bar{E}_s}{\bar{E}_f}\right)^{\frac{2}{3}}/2(1+\nu_f)\right]\right]} \quad (5)$$

The crumple height (h_c) was calculated to be 418 nm (2×*A*). We compared analytical values with experimental results. $\lambda_{c,x} \approx$ 277.67 nm estimated by the analysis of SEM images was closely matched with the analytically estimated value of 298 nm. The small discrepancy between the analytically calculated value and the experimental value is attributable to our assumption that AuNPs were not considered as a composite layer on graphene.

Determination of photoresponsivity

In order to compare photoresponsivity (R_{ph}) of photodetector devices, incident light power (P_{in}) of a λ_{light} = 532 nm diode laser through a 5x objective lens was measured. Photocurrents (I_{ph}) generated with respect to the incident light intensity was measured at $\varepsilon_{tensile,x}$ = 0%. The incident power was divided by 2 for photoresponsivity calculation, because only half of the laser beam illuminated a channel. The photoresponsivity ($R_{ph} = I_{ph} / (P_{in}/2)$) of a crumpled hybrid photodetector was estimated to be 0.0440 mA/W. For comparison, the photoresponsivity of a crumpled graphene photodetector and a flat graphene photodetector was calculated, same as that of the crumpled hybrid photodetector, and their respective photoresponsivity values were 0.0194 mA/W and 0.0034 mA/W.

Mechanical robustness test over cyclic strains

The mechanical robustness of the crumpled hybrid structure was tested by applying cycles of tensile strains between 0% and 200%. Optical extinction of a crumpled graphene-AuNPs hybrid structure was measured over one thousand cycles at varying tensile strains (Fig. S2). The mechanical robustness of a crumpled hybrid photodetector device was also tested. The photocurrent was measured with respect to one thousand cycles of the tensile strains at $\varepsilon_{tensile,x}$ = 100% (Fig. S5). To exclude viscoelastic behaviour of a VHB substrate, we conducted all the robustness tests with relaxation of a device for ~1 hour at every cycle.

Analysis of average size and number density of AuNPs

The average size and number density of AuNPs were estimated by image analysis with ImageJ[5] (Fig. S3). The SEM image of a flat graphene-AuNPs hybrid structure was cropped. The cropped image was transformed into an 8-bit image. Then, the area of particles and the number of particles were determined by ImageJ. The average diameter and the average number density ($\rho_{N,0}$) were 57.0±2.82 nm and 123±12.7 particles/μm^2 respectively. The average gap distance (d) was estimated to be 36.5 nm based on the image analysis of the post-processed images (see Fig. S3) of the SEM image (Fig. 2a). A simple particle arrangement model (Fig. S4) and the following equation was used for the estimation:

$$d = \frac{1\mu m - N_{1\mu m} \times D_{avg}}{N_{1\mu m} - 1} \quad (6)$$

where $N_{1\mu m}$ is the average number of particles in 1 μm, and D_{avg} is the average diameter of a particle. $N_{1\mu m}$ was calculated from the square root of the number density.

The number densities of AuNPs at $\varepsilon_{tensile,x}$ = 0% and 200% were estimated based on the average number density of flat graphene-AuNPs hybrid structure and the ratio of the crumpled surface area to the projected flat surface area (d_c) (Eq. 7) [6].

$$d_c = 1 + \frac{\pi^2 A^2}{2} \frac{{\lambda_{c,x}}^2 + {\lambda_{c,y}}^2}{{\lambda_{c,x}}^2 \cdot {\lambda_{c,y}}^2} \quad (7)$$

The values of d_c at $\varepsilon_{tensile,x}$ = 0% and 200% were calculated to be 5.23 and 4.10 respectively. The AuNPs number densities of crumpled hybrid structure under $\varepsilon_{tensile,x}$ = 0% and 200% were determined by multiplying the number density of the flat hybrid structure by the respective d_c values. Thus, the number densities of AuNPs in the crumpled hybrid structure at $\varepsilon_{tensile,x}$ = 0% and 200% were estimated to be 643.17 particles/μm^2 and 504.80 particles/μm^2 respectively.

Table S1. Comparison of the photoresponsivity (R_{ph}) of a hybrid photodetector with the crumpled graphene-AuNPs hybrid structure, a crumpled graphene photodetector, and a flat graphene photodetector. The photoresponsivity was determined with measured incident power of a λ_{light} = 532 nm laser light (P_{in}) and measured photocurrent (I_{ph}) respectively.

	P_{In}	I_{ph}	$R_{ph}(= I_{ph} /(P_{in}/2))$
Hybrid Structure	3.052 $X10^{-3}$ W	6.73 $X10^{-2}$ μA	0.0440 mA/W
Crumpled Graphene	3.105 $X10^{-3}$ W	3.01 $X10^{-2}$ μA	0.0194 mA/W
Flat Graphene	3.225 $X10^{-3}$ W	5.52 $X10^{-3}$ μA	0.0034 mA/W

Table S2. Comparison of normalized photocurrent ($I_{ph}/I_{ph,0}$) and normalized photoresponsivity ($R_{ph}/R_{ph,0}$) of a hybrid photodetector with the crumpled graphene-AuNPs hybrid structure, a crumpled graphene photodetector, and a flat graphene photodetector. $I_{ph,0}$ is the photocurrent of the hybrid photodetector measured at $\varepsilon_{tensile,x}$ = 0%, and $R_{ph,0}$ is the photoresponsivity of the hybrid photodetector determined at $\varepsilon_{tensile,x}$ = 0%.

	Hybrid Structure	**Crumpled Graphene**	**Flat Graphene**
$\boldsymbol{I_{ph}/I_{ph,0}}$	1	0.466	0.055
$\boldsymbol{R_{ph}/R_{ph,0}}$	1	0.440	0.078

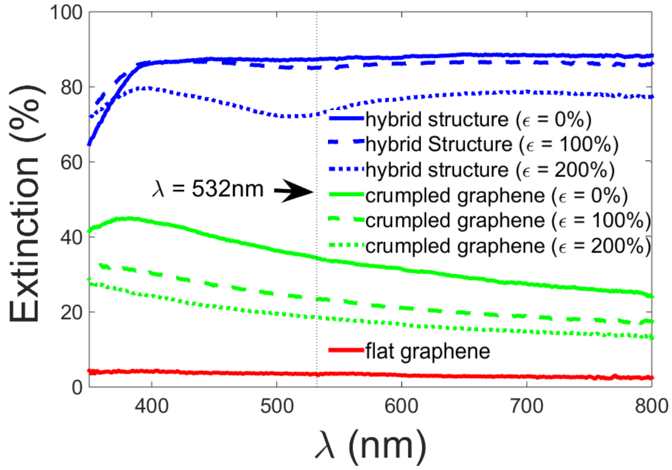

Fig. S1. Optical extinction spectra of a crumpled graphene-AuNPs hybrid structure and crumpled graphene at varying tensile strains of 0%, 100%, and 200%, and extinction spectrum of flat graphene (wavelength range between λ = 350-800 nm). The wavelength of 532 nm was denoted by a black dotted vertical line to indicate the relatively large difference of photo-absorption at $\varepsilon_{tensile,x}$ = 0% and 200% compared to other wavelengths.

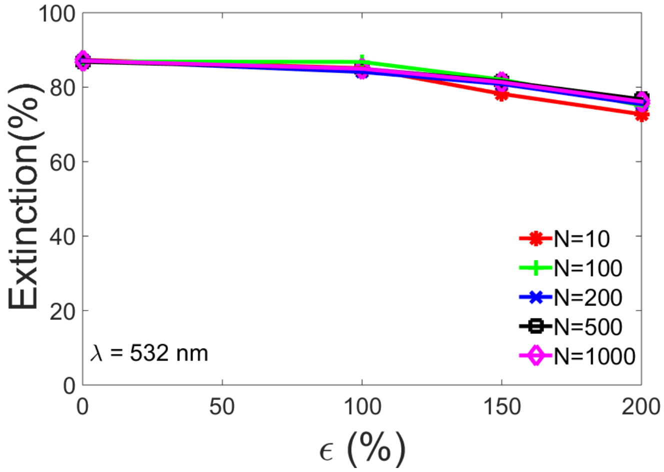

Fig. S2. Mechanical robustness of crumpled graphene-AuNPs hybrid structures. Measured optical extinction at λ_{light} = 532 nm at four different uniaxial strains (0%, 100%, 150%, and 200%) over 1000 cycles. The optical extinction was measured at 10th, 100th, 200th, 500th, and 1000th cycles.

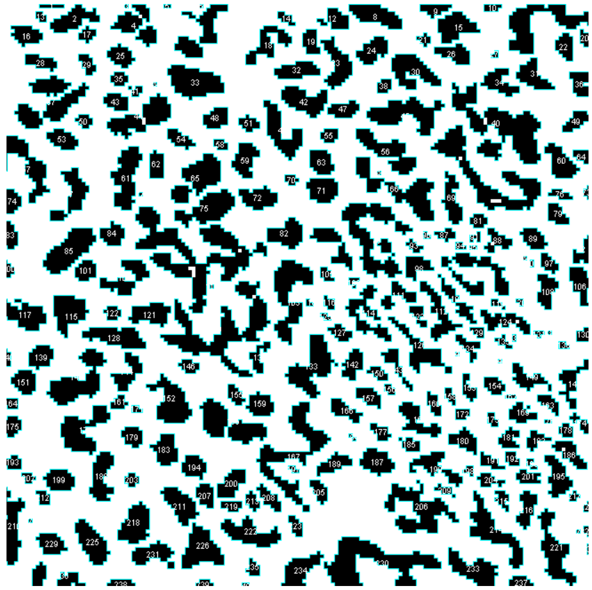

Fig. S3. Post-processed image of the SEM image for Au particle analysis. The SEM image of a flat graphene-AuNPs hybrid structure shown in Fig. 2a was post-processed for analysis of average size and number density of AuNPs by ImageJ.

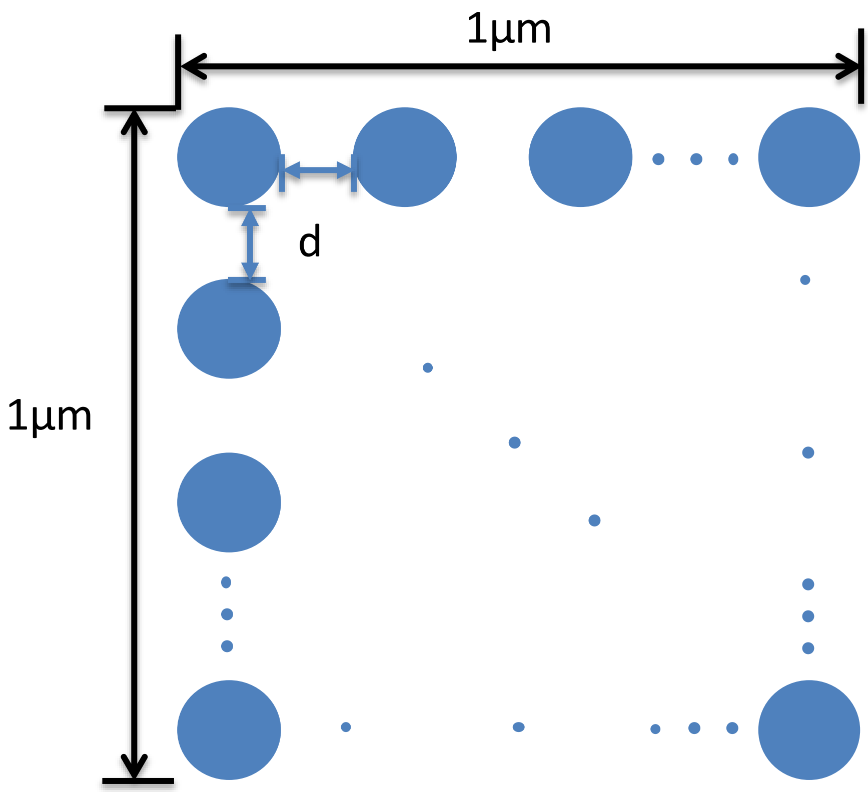

Fig. S4. Particle arrangement model for a particle gap distance, *d*. The distribution of AuNPs in a 1 µm×1 µm square is modelled as an ordered array to make an estimation of the gap distance (*d*) between particles.

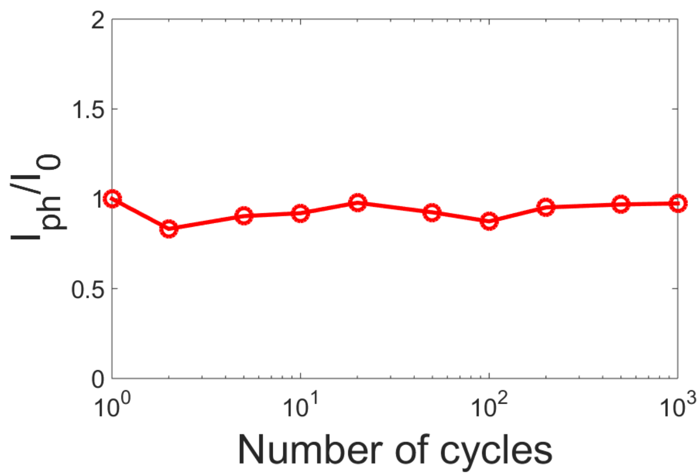

Fig. S5. Mechanical robustness of a stretchable photodetector based on crumpled graphene-AuNPs hybrid structures. Photocurrents were measured at $\varepsilon_{x,tensile}$ = 100% over one thousand cycles of stretching-relaxation. Measured photocurrents were normalized by the photocurrent measured at the first cycle (I_0).

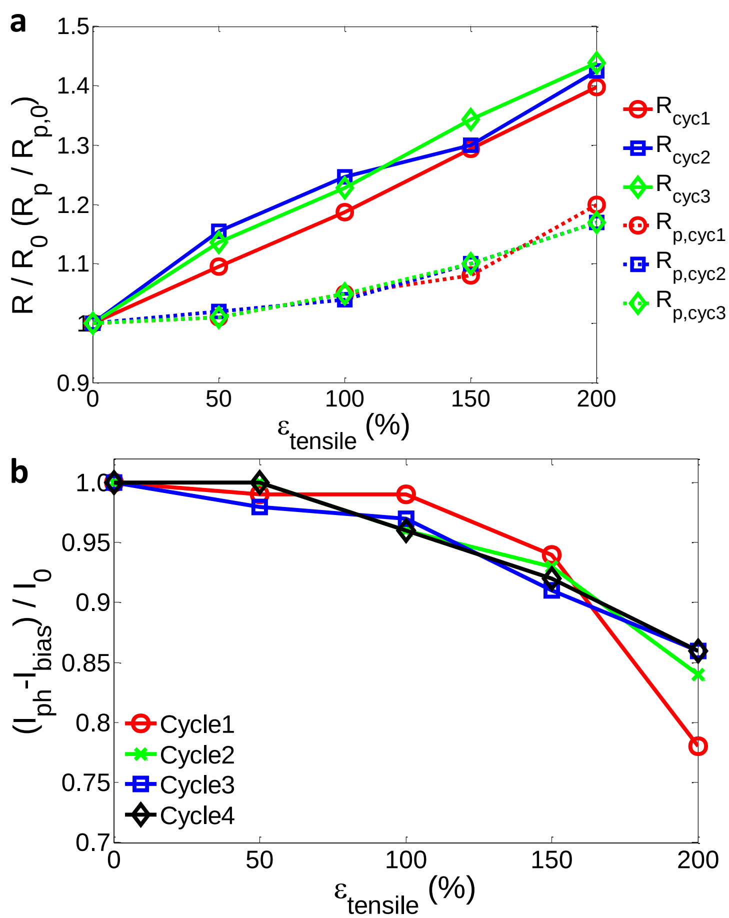

Fig. S6. Electrical characterizations of a stretchable photodetector based on crumpled graphene-AuNPs hybrid structures. (a) Resistance (R) and photoresistance (R_p = V_{bias} / I_{ph}, where I_{ph} is measured photocurrent and V_{bias} is bias voltage, 15 μV) measurements of the crumpled hybrid photodetector with multiple cycles of uniaxial tensile strains between 0% and 200%. Measured resistances and photoresistances were normalized by the resistance and photoresistance measured at $\varepsilon_{x,tensile}$ = 0% (R_0 and $R_{p,0}$), respectively. (b) Photocurrent (I_{ph} – I_{bias}) of the crumpled hybrid photodetector normalized by the photocurrent measured at $\varepsilon_{x,tensile}$ = 0% (I_0) with multiple cycles of uniaxial tensile strains between 0% and 200%. I_{bias} = V_{bias} / R, where R is measured resistance of the crumpled hybrid photodetector without light illumination.

Movie S1. Demonstration of a conformal photodetector with the crumpled graphene-AuNPs hybrid structure. This movie demonstrates dynamic photoresponse of the device, which is conformably integrated on the curved surface of a contact lens. The dynamic photocurrent is measured with three on-off cycles of a 532 nm laser light. The inset of the movie shows a high signal-to-noise ratio of the dynamic photocurrent, when the light is turned on and off in the second cycle.

Supplementary References

1. J. Song, H. Jiang, W. M. Choi, D. Y. Khang, Y. Huang, J. A. Rogers, *J. Appl. Phys.* 2008, **103**(1), 014303.
2. W. Bao, F. Miao, Z. Chen, H. Zhang, W. Jang, C. Dames, C. N. Lau, *Nat. Nanotechnol.* 2009, **4**(9), 562-566.
3. J. Zang, S. Ryu, N. Pugno, Q. Wang, Q. Tu, M. J. Buehler, X. Zhao, *Nat. Mater.* 2013, **12**(4), 321-325.
4. M. Bozlar, C. Punckt, S. Korkut, J. Zhu, C. Chiang Foo, Z. Suo, I. A. Aksay, *Appl. Phys. Lett.* 2012, **101**(9), 091907.
5. W. S. Rasband, ImageJ, U. S. National Institutes of Health, Bethesda, Maryland, USA, http://imagej.nih.gov/ij/, 1997-2016.
6. A. V. Thomas, B. C. Andow, S. Suresh, O. Eksik, J. Yin, A. H. Dyson, N. Koratkar, *Adv. Mater.* 2015, **27**(21), 3256-65.